REGULAR ARTICLE

Bonding in cationic MOH$_n^+$ (M = K − La, Hf − Rn; n = 0–2): DFT performances and periodic trends

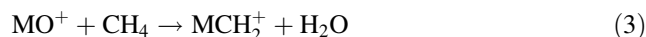Xinhao Zhang · Helmut Schwarz

Abstract The performances of the DFT functionals B3LYP, BHandHLYP, M06, M06-2X, PBE1PBE, TPSSh, X3LYP, and BP86 have been benchmarked with a thermochemistry database containing 50 bond dissociation energies (BDEs) of M–OH$_n^+$ complexes (n = 0–2). Among the tested methods, B3LYP was found to perform best both in accuracy and error distributions. Next, 162 BDEs (M$^+$–OH$_n$) (M = K − La, Hf − Rn; n = 0–2) are calculated at the B3LYP/def2-QZVP level of theory and their periodic trends are presented as an overview. Further, the H-atom affinities of MO$^+$ and MOH$^+$ are derived from the calculated BDEs.

Keywords Bond dissociation energy · M–O interaction · DFT · Benchmark · Periodic trends

1 Introduction

Oxides, hydroxides, and water complexes play important roles in catalysis, materials science, and biological systems. Knowledge of the bonding, especially the thermochemistry, of such species provides insight in understanding

X. Zhang (✉) · H. Schwarz (✉)
Institut für Chemie, Technische Universität Berlin, Straße des 17. Juni 135, 10623 Berlin, Germany
e-mail: Xinhao.Zhang@mail.chem.tu-berlin.de

H. Schwarz
e-mail: Helmut.Schwarz@mail.chem.tu-berlin.de
URL: http://www.chem.tu-berlin.de/

reaction mechanism, may help to improve catalytic processes and to design novel materials. For instance, metal oxides comprise an important class of catalysts in methane activation [1–3]. The model studies of the gas-phase reactions of CH$_4$ with gaseous metal-oxide MO$^+$ cations [4–12] reveal the existence of three reaction channels (Eqs. 1–3):

$$MO^+ + CH_4 \rightarrow M^+ + CH_3OH \qquad (1)$$

$$MO^+ + CH_4 \rightarrow MOH^+ + CH_3 \qquad (2)$$

$$MO^+ + CH_4 \rightarrow MCH_2^+ + H_2O \qquad (3)$$

Reaction (1) converts methane to methanol, reaction (2) is believed to constitute the crucial step in the oxidative coupling of methane, and formation of MCH$_2$ is of conceptual interest in the CH$_4$ → CH$_2$O conversion. For different MO$^+$, the branching ratios for reaction channels (1–3) largely depend on the thermochemistry, i.e. bond dissociation energy (BDE) of MO$^+$, MOH$^+$, or MCH$_2^+$. With a weak Ni–O bond, NiO$^+$ undergoes exclusively reaction channel (1) to transfer an O atom to CH$_4$ [13]. Channels (1) and (2) compete in the reaction between FeO$^+$ and methane [14–17]. Driven by the strong Pt=CH$_2^+$ bond, PtO$^+$ reacts with methane via channel (3) to give PtCH$_2^+$/H$_2$O [18, 19]. Due to their wide applications, transition metal oxides have formed the subject of numerous experimental and theoretical studies [20–29]. In contrast, main-group element oxides have received much less attention. However, methane activation by the main-group element oxides, e.g. MgO$^+$ [30], MO$^+$ (M = Ca, Sr or Ba) [31], [(Al$_2$O$_3$)$_x$]$^+$ [32], SO$_2^+$ [33], P$_4$O$_{10}^+$ [34], and PbO$^+$ [35], has demonstrated recently the unexpected potential of s- and p-block element oxides.

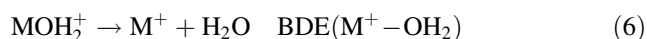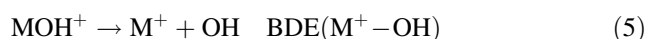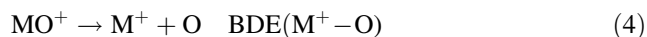Given the lack of experimentally derived BDEs of the M–O bonds in MOH$_n^+$ (n = 0–2) for most of the main-

group elements and also for many transition metals, here we present a systematic theoretical study of the bonding of MOH_n^+ (M = K − La, Hf − Rn; n = 0–2). In the first part of this work, we benchmark the performance of eight density-functional theory (DFT) methods, i.e. B3LYP [36–38], BHandHLYP [39], M06 [40], M06-2X [41], PBE1PBE [41], TPSSh [42], X3LYP [43], and BP86 [44]. After being validated by a comparison with experimental data, the most reliable method is used to predict the BDEs for MOH_n^+ (Eqs. 4–6) in the second part. Finally, based on the calculated BDEs, periodic trends in bonding of M–OH_n^+ and new thermochemical information are presented.

$$MO^+ \rightarrow M^+ + O \quad BDE(M^+ - O) \tag{4}$$

$$MOH^+ \rightarrow M^+ + OH \quad BDE(M^+ - OH) \tag{5}$$

$$MOH_2^+ \rightarrow M^+ + H_2O \quad BDE(M^+ - OH_2) \tag{6}$$

2 Computational details

2.1 Database for benchmark

To achieve a "mindless DFT benchmarking" which aims at excluding chemical biases and providing a more "universal" survey, Korth and Grimme proposed a diversity-oriented approach to generate thermochemical benchmark sets [45]. Toward the same goal, we adopted a different strategy to address the "selection" problem by making *no selections*, including almost *all* of the experimental data currently available in the field. A database of 50 BDEs for MOH_n^+ (n = 0–2) was constructed from the experimental data. It is composed of 32 MOH_n^+ systems from the 4th, 9 MOH_n^+ from the 5th, and 9 MOH_n^+ from the 6th row. In terms of the ligands O, OH and OH_2, the database contains 26 MO^+, 11 MOH^+, and 13 MOH_2^+ examples. Moreover, 28 different metals M, mostly transition metals, are included. Details of these 50 BDEs are presented in the Tables 4, 5, 6, given in the next section. Most of the experimental data are derived from guided ion beam (GIB) mass spectrometry-based measurement performed in Armentrout's laboratory [46], on the ground that (1) GIB studies have proven quite reliable for deriving thermochemical data and have provided a large set of internally consistent data [47, 48], (2) discrepancies that may arise from using between different experimental techniques (e.g., collision induced dissociation or photodissociation) are avoided; thus, the systematic errors are minimized.

2.2 Methods

The accuracy of DFT for describing metal–ligand interactions has been benchmarked by different groups [49–57]. Many of these studies concluded that hybrid

DFT methods, especially B3LYP, are best suited to account for the energetics of transition metal complexes [58–60]. However, B3LYP has also been reported to be incapable to describe some of the systems and, consequently, new functionals have been developed [61–70]. Here, we focus on the M–O interaction and we set out to probe if B3LYP is suitable to describe these systems properly. Therefore, we evaluated the performance of eight DFT functionals: B3LYP, BHandHLYP, M06, M06-2X, PBE1PBE, TPSSh, X3LYP, and BP86. Seven of them are hybrid functionals and the classic BP86 is chosen as a representative of a non-hybrid functional for comparison. For all eight functionals, the def2-QZVP basis sets [71], in which effective core potential (ECP) was used for 5th and 6th row elements [72–76], were employed. In addition, two other popular basis sets are used for B3LYP to examine the role of basis set effects. These two are denoted as BS-LA (Lanl2dz with ECP for M and 6-31G(d,p) for O and H) and BS-SDD (SDD with ECP for M and 6-31G(d,p) for O and H) [76].

In addition, all possible spin multiplicities were calculated for every MOH_n^+ species investigated. For each spin state, geometry optimizations were started with at least three different initial structures, taking symmetry, bond length, etc., into account. In most cases, the eight functionals employed predict the same ground state for a given species. However, for systems having energetically comparable low-lying states, the different functionals assign different spin states to the ground state. As the energies of these near-degenerate states are rather close, the energetics between different states do not affect dramatically the BDE calculations. Frequencies were computed for all optimized structures with the corresponding optimization methods. Zero-point energy (ZPE) corrections were added without any scaling. For atomic cations M^+, the ground states were examined by comparing with experiments [22]. All calculations were carried out by using the Gaussian 09 package [77].

3 Results and discussion

3.1 Benchmark

3.1.1 Performance for elements from different periods of the periodic table

The various errors of BDEs for the 4th, 5th, and 6th row MOH_n^+ complexes are given in Table 1. Mean absolute error (MAE), mean error (ME), maximum error (E_{max}), minimum error (E_{min}), and root-mean-square deviation (rmsd) were chosen as parameters to evaluate the performance of the eight density functionals.

Table 1 Errors (kJ mol^{-1}) for the BDEs of the 4th, 5th, and 6th row MOH$_n^+$ complexes

Method[a]	MAE	ME	E_{max}	E_{min}	rmsd
4th row					
B3LYP/def2-QZVP	17	−4	46	−65	22
B3LYP/BS-LA	48	−14	127	−205	71
B3LYP/BS-SDD	35	2	63	−181	51
BHandHLYP	63	−60	22	−209	63
M06	29	−8	54	−124	38
M06-2X	36	−22	36	−151	47
PBE1PBE	23	−11	38	−103	29
TPSSh	20	10	59	−44	23
X3LYP	18	−4	46	−71	24
BP86	41	39	116	−20	31
5th row					
B3LYP/def2-QZVP	17	−13	11	−60	19
B3LYP/BS-LA	82	−67	52	−203	80
B3LYP/BS-SDD	23	−17	29	−54	21
BHandHLYP	103	−103	−12	−165	54
M06	25	10	45	−51	28
M06-2X	33	−29	12	−81	31
PBE1PBE	20	−20	−1	−75	21
TPSSh	14	−5	11	−68	23
X3LYP	18	−16	7	−62	19
BP86	58	58	115	1	38
6th row					
B3LYP/def2-QZVP	25	9	36	−59	29
B3LYP/BS-LA	78	−42	61	−278	120
B3LYP/BS-SDD	17	−2	34	−46	22
BHandHLYP	79	−79	−29	−119	26
M06	25	16	73	−28	32
M06-2X	28	−15	29	−59	27
PBE1PBE	20	0	29	−46	25
TPSSh	27	18	55	−33	25
X3LYP	24	7	34	−59	28
BP86	85	79	114	−29	47

[a] The def2-QZVP basis sets with ECP are used unless otherwise noted

With the same def2-QZVP basis sets, the functionals B3LYP, PBE1PBE, TPSSh, and X3LYP give similar MAEs of around 20 kJ mol^{-1}; for M06 and M06-2X, the MAEs are a slightly larger centering around 30 kJ mol^{-1}; BP86 performs much worse than the above hybrid functionals in two aspects: the MAEs are larger and the MAEs increase dramatically from the 4th row down to the 6th row; finally, BHandHLYP exhibits the largest MAE up to 103 kJ mol^{-1}. The large MAE of BHandHLYP for the MOH$_n^+$ system is somewhat surprising, because this method performed much better than B3LYP for describing the BDEs of various MCH$_3^+$ systems [49]. On the other

hand, the MAEs of BHandHLYP are consistent with Truhlar's benchmark study using the MLBE21/05 database [54]. When a large proportion of M–OH$_n$ complexes were included in the database, BHandHLYP was also found to have the largest MAE of ca. 80 kJ mol^{-1} in the BDE calculations [54]. This indicates that BHandHLYP is not appropriate for describing the M–O bonding systems, and a universally applicable functional does not seem to exist. Two other popular basis sets were used for the B3LYP calculations. Only for the 6th row complexes MOH$_n^+$, BS-SDD gives a smaller MAE than those obtained in the def2-QZVP calculations. For other cases, BS-LA and BS-SDD cannot compete with def2-QZVP. The rather poor performance of BS-LA is largely due to their neglecting d- and f-functions for main-group elements [78] and transition metals [79], respectively. In particular, for BDE(Ca$^+$–O), BDE(Ca$^+$–OH), BDE(Sr$^+$–O), BDE(Sr$^+$–OH), BDE(Ba$^+$–O), and BDE(Ba$^+$–OH), B3LYP/BS-LA results in errors as large as −205, −169, −203, −192, −246, and −278 kJ mol^{-1}, respectively. Thus, caution is indicated to use Lanl2dz to describe the alkaline-earth element bond energies to O and OH ligands, without including d-functions.

The negative MEs further show that most of the tested hybrid DFT methods, especially BHandHLYP, tend to underestimate BDE. This effect is less pronounced for the 6th row MOH$_n^+$. In contrast, BP86 tends to overestimate BDE.

E_{max}, E_{min}, and rmsd indicate the error spread of each method. B3LYP, PBE1PBE, TPSSh, and X3LYP are comparable to each other. Furthermore, these four functionals with def2-QZVP basis set perform constantly well as indicated by both MAE and rmsd for all complexes from the three periods, thus showing that the relativistic effects [80–85] are well described for the 5th and 6th row elements by the ECPs. On the other hand, ignoring the effects of relativity for the 4th row elements does not affect much the binding energy calculation either. This may suggest fortuitous error compensation.

3.1.2 Performance for different ligand systems

The errors for the BDEs of different ligand systems, i.e. oxides (MO$^+$), hydroxides (MOH$^+$), and water complexes (MOH$_2^+$) are listed in Table 2. The data in Table 2 clearly reveals the origin of the errors. Hybrid DFT methods often underestimate BDEs because exact exchange favors high-spin over low-spin states, i.e. atomic cations and dissociated ligands versus ligated complexes. With the smallest fraction of exact exchange, i.e. 10%, among all the tested hybrid functionals, TPSSh is the only hybrid functional which overestimates BDEs, thus giving positive MEs, for the three MOH$_n^+$ ($n = 0$–2) systems. For all other hybrid

functionals tested, due to the preference for the high-spin atomic cation and the open-shell triplet O atom (or the doublet OH), most of the MEs of BDE(M^+–O) and BDE(M^+–OH) are negative. For the water complexes MOH_2^+, dissociation of the singlet water ligand hardly affects the spin state of the system. Therefore, for this system positive MEs are obtained for most of the functionals except BHandHLYP. As expected, the non-hybrid functional BP86 results in overbinding for all systems. Interestingly, BHandHLYP performs worst for BDE(M^+–O) and best for BDE(M^+–OH_2), as shown in Table 2. Not as poor are the performances of M06 and M06-2X in calculating the BDE(M^+–O). B3LYP, PBE1PBE, TPSSh, and X3LYP exhibit reasonable accuracy for all three MOH_n^+ ($n = 0$–2) systems. More importantly, as seen from E_{max}, E_{min}, and rmsd, the error spread of these four functionals are rather narrow, implying that these functionals may be suitable in calculating relative energies because of the cancelation of the systematic errors. This is important for those calculations that involve two-state-reactivity scenarios [86–92], e.g. reactions with O_2 [93–103].

3.1.3 Overall performance

In Table 3, we summarize the overall performance of the eight functionals tested for calculating the BDEs of MOH_n^+, and in Fig. 1, the mean error (ME) of 50 BDEs is plotted as a function of the fraction of exact exchange (mixing coefficients of HF-exchange, X). Excluding M06 and M06-2X, one obtains a linear relationship (with $R^2 = 0.9746$) between the ME and the exact exchange admixture of the remaining five hybrid functionals tested and the non-hybrid BP86 (X = 0%). Reiher and co-workers reported that the energy splitting between different spin states of Fe(II)-sulfur complexes depends linearly on the exact exchange admixture parameter c3 [104]. In the present work, the hybrid DFT preference on the high-spin states (right sides of Eqs. 4 and 5) was reflected by the mean error in calculating the BDEs. Even for a relatively large test set containing as many as 50 BDEs, a linear relationship exists. To achieve ME = 0 in predicting the BDEs of MOH_n^+, an admixture of ca.18% is suggested; this value is close to the optimal range of 10–15% as proposed by Reiher et al. [104]. As shown in Fig. 1, M06 and M06-2X do not fit the linear relationship, thus indicating that the preference of HF-exchange on high-spin states was somehow compensated in the functional design [40, 65–67].

Concerning the accuracy, the non-hybrid BP86 functional performs worst when compared to all tested hybrid functionals except BHandHLYP. M06 and M06-2X give much better results than BHandHLYP, but are not as good as the other four hybrid functionals. Although M06 was parameterized for transition metal and nonmetal systems

Table 2 Errors (kJ mol^{-1}) for the BDEs of different ligand systems MO^+, MOH^+, and MOH_2^+

| Method[a]	MAE	ME	E_{max}	E_{min}	rmsd
MO^+					
B3LYP/def2-QZVP	20	−6	36	−65	25
B3LYP/BS-LA	65	−46	61	−246	82
B3LYP/BS-SDD	32	−25	34	−181	43
BHandHLYP	111	−111	−29	−209	48
M06	33	−1	73	−124	45
M06-2X	49	−44	29	−151	45
PBE1PBE	26	−19	29	−103	29
TPSSh	19	7	55	−68	24
X3LYP	21	−10	34	−71	25
BP86	75	75	116	13	31
MOH^+					
B3LYP/def2-QZVP	20	−10	16	−59	23
B3LYP/BS-LA	78	−61	45	−278	100
B3LYP/BS-SDD	15	2	47	−46	22
BHandHLYP	60	−60	−25	−90	22
M06	28	−1	54	−45	32
M06-2X	18	−10	16	−38	18
PBE1PBE	23	−14	20	−51	24
TPSSh	23	8	41	−33	26
X3LYP	20	−10	15	−59	22
BP86	39	34	85	−29	27
MOH_2^+					
B3LYP/def2-QZVP	15	9	46	−25	18
B3LYP/BS-LA	34	34	127	2	31
B3LYP/BS-SDD	39	39	63	9	16
BHandHLYP	9	−2	22	−28	12
M06	14	1	54	−32	21
M06-2X	16	12	36	−18	16
PBE1PBE	13	9	38	−23	16
TPSSh	19	14	59	−22	23
X3LYP	16	11	46	−23	18
BP86	17	13	65	−20	20

[a] The def2-QZVP basis sets with ECP are used unless otherwise noted

while M06-2X was designed for the main-group thermochemistry, the difference between M06 and M06-2X in calculating BDEs of MOH_n^+ is not very significant. For our database containing 28 metals, the performance of M06-2X is still acceptable. Within the rather small energy regime of only a few kJ mol^{-1}, it is difficult to conclude which functional performs best among B3LYP, PBE1PBE, TPSSh, and X3LYP. Considering the accuracy (MAE and ME), the error distribution (E_{max} − E_{min}, and rmsd), and the excellent performance of B3LYP/def2-QZVP in predicting BDE(M^+–CH_2) (M = K − La, Hf − Rn) [105],

Table 3 Errors (kJ mol^{-1}) for the BDEs of the whole test set

Method[a]	MAE	ME	E_{max}	E_{min}	rmsd
B3LYP/def2-QZVP	19	−3	46	−65	24
B3LYP/BS-LA	60	−29	127	−278	86
B3LYP/BS-SDD	30	−2	63	−181	43
BHandHLYP	73	−71	22	−209	59
M06	27	0	73	−124	37
M06-2X	34	−22	36	−151	42
PBE1PBE	22	−11	38	−103	28
TPSSh	20	9	59	−68	24
X3LYP	19	−4	46	−71	25
BP86	52	50	116	−29	39

[a] The def2-QZVP basis sets with ECP are used unless otherwise noted
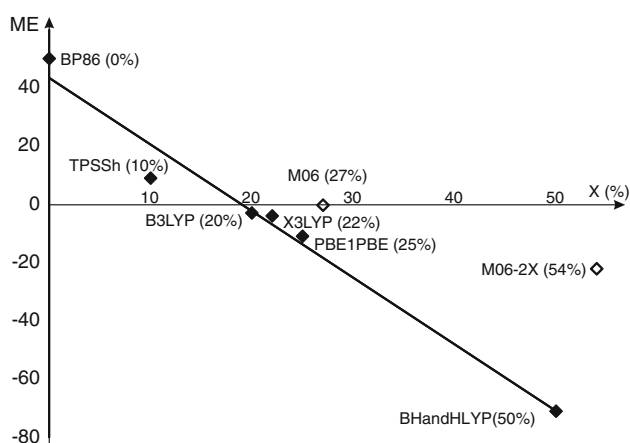
Fig. 1 Correlation between the ME (kJ mol^{-1}) and the percentage of exact exchange (X, %) of functionals

we chose this method for the following calculations of the MOH_n^+ complexes (M = K − La, Hf − Rn; $n = 0$–2).

3.2 Bond dissociation energy

3.2.1 Theoretically derived BDEs

Tables 4, 5, and 6 list the spin multiplicities of the ground states (2S + 1), the bond distances of M–O ($d_{M–O}$), the BDEs calculated at B3LYP/def-QZVP (BDE_{b3lyp}) as well as the experimental BDEs (BDE_{exp}) of MOH_n^+ (M = K − La, Hf – Rn; $n = 0$–2). All the BDE_{exp} shown in Tables 4, 5, and 6, except for $BDE(Pd^+–O)_{exp}$ and $BDE(Ag^+–O)_{exp}$, constituted the database for our benchmarking. Before turning to the thermochemistry, let us take a glance at the geometries. For MO^+ and MOH^+, most of the calculated M–O bond lengths, $d_{M–O}$, are in good agreement with data derived from Pyykkö's covalent radii approach [106–108]. The $d_{M–O}$ of MO^+ refers to a double bonded radii model [107], and the $d_{M–O}$ of MOH^+ refer to a single bonded radii model [108]. There are two exceptions: the $d_{M–O}$ of groups 1 and 13 is longer, and the $d_{M–O}$ of M–Oes 4–6 list the ground states, bond distance of M–OE groups 2–6 is shorter than those based on the covalent radii model. The lengthening is due to the fact that group 1(ns^0) and group 13 (np^0) M^+ cations cannot offer valence electron to form strong covalent interactions with an O atom or an OH radical. On the other hand, shortening of the M–O bonds is a consequence of the ionic bonding character and the empty d orbital of M^+ that enhances the M–O interaction. The MO bonds for the early transition metal MO^+ cations were proposed to correspond to a triple bond [109–113]. Indeed, our calculated $d_{M–O}$ for group 2–6 are close to those derived from the triple bonded radii model [106].

The largest absolute error in Tables 4, 5 and 6 amounts to 65 kJ mol^{-1} for BDE(Cr^+–O). Various BDE(Cr^+–O) values, i.e. 340 [24], 303 [25], 289 [26], 294(def2-QZVP), 251(BS-LA), and 312(BS-SDD) kJ mol^{-1}, respectively, have been calculated at B3LYP with different basis sets. Although Miliordos and Mavridis have demonstrated that incorporation of scalar relativistic and core correlation effects improved the performance of MRCI in calculating BDE(Cr^+–O) [113], the origin of the error of B3LYP for Cr is not yet completely understood [136]. Another large absolute error (60 kJ mol^{-1}) concerns the BDE(Zr^+–O). However, in this case, the BDE(Zr^+–O)$_{exp}$ seems to fall out of the trends that are regarded as representative for neighboring oxides in the periodic table. Therefore, a deeper theoretical analysis as well as independent measurements is indicated before definitive conclusions about the quality of the present DFT calculation should be made.

When comparing the theoretical and experimental thermochemical data, one encounters challenges not only for the B3LYP calculations [137] but also the experimental results. For instance, large discrepancies between BDE_{b3lyp} and BDE_{exp} were reported for PdO^+ and AgO^+, and the BDE(Pd^+–O) and BDE(Ag^+–O) have not been included in our database because there are good reasons to be skeptical about the quality of the experimental results. The BDE(Pd^+–O)$_{exp}$ and BDE(Ag^+–O)$_{exp}$ were determined from the kinetic energy onset for the formation of MO^+ in the ion–molecule reaction (IMR) of M^+ with O_2. The IMR of Pd^+ with O_2 was assigned to a direct mechanism, while the reaction of Ag^+ with O_2 was interpreted in terms of an impulsive pairwise mechanism [120]. However, in reality, both reactions may well occur via these two mechanisms in a competitive fashion. As a result, when only one of the mechanisms is taken into account, the BDE(Pd^+–O)$_{exp}$ is underestimated and the BDE(Ag^+–O)$_{exp}$ is overestimated; a BDE(Ag^+–O)$_{exp}$ of 119 ± 8 kJ mol^{-1} has been

Table 4 Computed ground states (2S + 1), bond distances of M–O (d_{M-O}, in Å), BDEs (BDE$_{b3lyp}$, in kJ mol^{-1}) and experimental BDEs (BDE$_{exp}$, in kJ mol^{-1}) of MO$^+$

	2S + 1[a]	d_{M-O}	BDE$_{b3lyp}$	BDE$_{exp}$		2S + 1[a]	d_{M-O}	BDE$_{b3lyp}$	BDE$_{exp}$		2S + 1[a]	d_{M-O}	BDE$_{b3lyp}$	BDE$_{exp}$
KO$^+$	3/1	2.974	17		RbO$^+$	3/1	3.201	13		CsO$^+$	3/1	3.466	10	
CaO$^+$	2/2	1.873	340	344 ± 5[b]	SrO$^+$	2/2	1.997	323	335 ± 6[f]	BaO$^+$	2/2	2.100	380	396 ± 19[j]
ScO$^+$	1/3	1.612	658	689 ± 6[c]	YO$^+$	1/1	1.745	679	699 ± 17[g]	LaO$^+$	1/3	1.856	727	
TiO$^+$	2/4	1.565	646	664 ± 7[c]	ZrO$^+$	2/4	1.681	689	749 ± 11[g]	HfO$^+$	2/2	1.700	692	667 ± 11[k]
VO$^+$	3/5	1.560	541	564 ± 15[c]	NbO$^+$	3/5	1.648	695	688 ± 17[g]	TaO$^+$	3/5	1.669	713	685 ± 12[k]
CrO$^+$	4/6	1.592	294	359 ± 12[c]	MoO$^+$	4/6	1.623	499	488 ± 2[g]	WO$^+$	4/6	1.642	689	653 ± 7[k]
MnO$^+$	5/7	1.729	268	285 ± 13[c]	TcO$^+$	3/7	1.629	382		ReO$^+$	5/7	1.679	428	427 ± 71[l]
FeO$^+$	6/6	1.637	336	335 ± 6[c]	RuO$^+$	4/4	1.669	353	368 ± 5[h]	OsO$^+$	6/6	1.729	433	418 ± 51[m]
CoO$^+$	5/3	1.635	308	314 ± 5[c]	RhO$^+$	3/3	1.651	280	291 ± 6[h]	IrO$^+$	5/5	1.724	415	
NiO$^+$	4/2	1.638	224	264 ± 5[c]	PdO$^+$	2/2	1.782	207	*141 ± 11*[h,i]	PtO$^+$	4/2	1.735	328	315 ± 7[n]
CuO$^+$	3/1	1.792	131	130 ± 12[d]	AgO$^+$	3/1	2.194	64	*119 ± 5*[h,i]	AuO$^+$	3/1	1.892	144	108 ± 8[o]
ZnO$^+$	2/2	1.803	157	161 ± 5[e]	CdO$^+$	2/2	2.009	110		HgO$^+$	2/2	1.999	96	
GaO$^+$	3/1	1.907	30		InO$^+$	3/1	2.208	12		TlO$^+$	3/1	2.988	0	
GeO$^+$	2/2	1.655	346		SnO$^+$	2/2	1.860	285		PbO$^+$	2/2	1.966	242	
AsO$^+$	1/3	1.565	616		SbO$^+$	1/3	1.762	495		BiO$^+$	1/3	1.853	428	
SeO$^+$	2/4	1.579	404		TeO$^+$	2/4	1.765	333		PoO$^+$	2/4	1.862	279	
BrO$^+$	3/3	1.637	394		IO$^+$	3/3	1.801	338		AtO$^+$	3/3	1.901	295	
KrO$^+$	2/2	1.798	210		XeO$^+$	2/2	1.924	185		RnO$^+$	2/2	2.012	168	

[a] State of MO$^+$/state of M$^+$. The atomic ground states are consistent with experiments [22]. Details of electron configuration and total energy of atomic cations are available in supplementary material; [b] [114]; [c] [115]; [d] [116]; [e] [117]; [f] [118]; [g] [119]; [h] [120]; [i] not included in test set; [j] [121]; [k] [122]; [l] [123]; [m] [124]; [n] [125]; [o] [126]

Table 5 Computed ground states (2S + 1), bond distances of M–O (d_{M-O}, in Å), BDEs (BDE$_{b3lyp}$, in kJ mol^{-1}) and experimental BDEs (BDE$_{exp}$, in kJ mol^{-1}) of MOH$^+$

	2S + 1	d_{M-O}	BDE$_{b3lyp}$	BDE$_{exp}$		2S + 1	d_{M-O}	BDE$_{b3lyp}$	BDE$_{exp}$		2S + 1	d_{M-O}	BDE$_{b3lyp}$	BDE$_{exp}$
KOH$^+$	2	2.677	47		RbOH$^+$	2	2.886	40		CsOH$^+$	2	3.086	36	
CaOH$^+$	1	1.892	457	444 ± 29[a]	SrOH$^+$	1	2.023	428	444 ± 19[a]	BaOH$^+$	1	2.144	472	531 ± 19[a]
ScOH$^+$	2	1.766	471	499 ± 9[b]	YOH$^+$	2	1.894	538		LaOH$^+$	2	2.032	518	
TiOH$^+$	3	1.738	473	465 ± 12[b]	ZrOH$^+$	3	1.829	546		HfOH$^+$	1	1.804	547	
VOH$^+$	4	1.728	406	434 ± 14[b]	NbOH$^+$	4	1.786	490		TaOH$^+$	4	1.782	525	
CrOH$^+$	5	1.751	267	298 ± 14[c]	MoOH$^+$	5	1.846	323		WOH$^+$	5	1.814	468	
MnOH$^+$	6	1.754	323	332 ± 24[c]	TcOH$^+$	6	1.852	348		ReOH$^+$	6	1.844	336	
FeOH$^+$	5	1.716	371	366 ± 12[d]	RuOH$^+$	5	1.877	249		OsOH$^+$	5	1.839	323	
CoOH$^+$	4	1.726	316	302 ± 4[e]	RhOH$^+$	4	1.875	214		IrOH$^+$	4	1.839	332	
NiOH$^+$	3	1.707	252	236 ± 19[b]	PdOH$^+$	3	1.876	188		PtOH$^+$	3	1.841	277	
CuOH$^+$	2	1.801	162		AgOH$^+$	2	2.200	95		AuOH$^+$	2	1.976	152	
ZnOH$^+$	1	1.765	228		CdOH$^+$	1	1.970	168		HgOH$^+$	1	1.984	150	
GaOH$^+$	2	1.788	102		InOH$^+$	2	2.067	61		TlOH$^+$	2	2.763	47	
GeOH$^+$	1	1.672	504		SnOH$^+$	1	1.875	426		PbOH$^+$	1	1.998	375	
AsOH$^+$	2	1.691	451		SbOH$^+$	2	1.889	384		BiOH$^+$	2	1.998	340	
SeOH$^+$	1	1.700	342		TeOH$^+$	3	1.886	301		PoOH$^+$	3	1.997	266	
BrOH$^+$	2	1.732	343		IOH$^+$	2	1.902	292		AtOH$^+$	2	2.006	260	
KrOH$^+$	1	1.847	262		XeOH$^+$	1	1.973	224		RnOH$^+$	1	2.057	205	

[a] [121]; [b] [127]; [c] [115]; [d] [128]; [e] [129]

suggested as a preliminary value [120]. Also, a theoretical paper called for a revision of the BDE(Ag$^+$–O)$_{exp}$, and a BDE(Ag$^+$–O) = 45 kJ mol^{-1}, calculated at CCSD(T), has

been reported [138]. For PdO$^+$, our recent work on the methane activation by MO$^+$ (M = Ni, Pd, Pt) [13] indicated that the BDE(Pd$^+$–O)$_{exp}$ (141 kJ mol^{-1}) [120] is too

Table 6 Computed ground states $(2S + 1)$, bond distances of M–O $(d_{M-O}$, in Å), BDEs $(BDE_{b3lyp}$, in kJ mol$^{-1})$ and experimental BDEs $(BDE_{exp}$, in kJ mol$^{-1})$ of MOH_2^+

	$2S+1$	d_{M-O}	BDE_{b3lyp}	BDE_{exp}		$2S+1$	d_{M-O}	BDE_{b3lyp}	BDE_{exp}		$2S+1$	d_{M-O}	BDE_{b3lyp}	BDE_{exp}
KOH_2^+	1	2.622	68	71[a]	$RbOH_2^+$	1	2.823	58		$CsOH_2^+$	1	3.005	51	
$CaOH_2^+$	2	2.299	117	121[b]	$SrOH_2^+$	2	2.493	95		$BaOH_2^+$	2	2.658	89	
$ScOH_2^+$	3	2.169	155	131[c]	YOH_2^+	1	2.237	145		$LaOH_2^+$	3	2.507	123	
$TiOH_2^+$	4	2.098	177	154 ± 6[d]	$ZrOH_2^+$	4	2.197	139		$HfOH_2^+$	2	2.144	139	
VOH_2^+	5	2.066	154	147 ± 5[d]	$NbOH_2^+$	5	2.141	166		$TaOH_2^+$	5	2.123	152	
$CrOH_2^+$	6	2.080	139	129 ± 9[d]	$MoOH_2^+$	6	2.186	138		WOH_2^+	6	2.119	202	
$MnOH_2^+$	7	2.178	118	119 ± 6[d]	$TcOH_2^+$	5	2.150	104		$ReOH_2^+$	7	2.431	95	
$FeOH_2^+$	4	2.002	174	128 ± 5[e]	$RuOH_2^+$	4	2.171	140		$OsOH_2^+$	4	2.084	108	
$CoOH_2^+$	3	1.967	193	161 ± 6[d]	$RhOH_2^+$	3	2.165	143		$IrOH_2^+$	3	2.071	179	
$NiOH_2^+$	2	1.946	181	180 ± 3[d]	$PdOH_2^+$	2	2.188	129		$PtOH_2^+$	2	2.096	185	
$CuOH_2^+$	1	1.942	168	157 ± 8[d]	$AgOH_2^+$	1	2.217	125	131 ± 8[f]	$AuOH_2^+$	1	2.153	157	
$ZnOH_2^+$	2	2.055	138	163[c]	$CdOH_2^+$	2	2.315	107		$HgOH_2^+$	2	2.379	111	
$GaOH_2^+$	1	2.254	98		$InOH_2^+$	1	2.496	80		$TlOH_2^+$	1	2.616	73	
$GeOH_2^+$	2	2.061	166		$SnOH_2^+$	2	2.295	131		$PbOH_2^+$	2	2.419	117	
$AsOH_2^+$	3	2.013	218		$SbOH_2^+$	3	2.226	171		$BiOH_2^+$	3	2.340	153	
$SeOH_2^+$	2	1.912	129		$TeOH_2^+$	2	2.122	84		$PoOH_2^+$	4	2.774	68	
$BrOH_2^+$	1	1.912	231		IOH_2^+	1	2.108	157		$AtOH_2^+$	1	2.214	128	
$KrOH_2^+$	2	2.465	258		$XeOH_2^+$	2	2.583	165		$RnOH_2^+$	2	2.631	138	

[a] [130]; [b] [131]; [c] [132]; [d] [133]; [e] [134]; [f] [135]

low and does not fit the periodic trends noted [13]. Furthermore, comparing the $BDE(Ni^+-S)_{exp}$ (237 kJ mol^{-1}) [139] with the $BDE(Pd^+-S)_{exp}$ (228 kJ mol^{-1}) [140], and the $BDE(Ni^+-CH_2)_{exp}$ (308 kJ mol^{-1}) [141] with the $BDE(Pd^+-CH_2)_{exp}$ (284 kJ mol^{-1}) [46], the $BDE(Pd^+-O)$ is expected to be close to the $BDE(Ni^+-O)$ (264 kJ mol^{-1}) [115]. Here, the inconsistencies between theory and experiment reveal an interesting interplay: while theory is validated by experiment, it also suggests an experimental re-investigation [142, 143]. A similar situation has been met for the intriguing case of $BDE(Pd^+-CH_2I)$ [144]. /Para>For those $BDEs(M^+-OH_n)$ for which no experimental data are at hand, we recommend our predicted BDEs as a reference. For example, the BDE ($Cu^+-OH)_{exp}$ has not been measured yet. We predict the BDE $(Cu^+-OH)_{b3lyp}$ (162 kJ mol^{-1}) to be slightly lower than the BDE $(Cu^+-OH_2)_{b3lyp}$ (168 kJ mol^{-1}). This trend is in agreement with a collisionally activated dissociation study of $[Cu(OH)(H_2O)]^+$ in which the loss of OH is slightly favored over the evaporation of H_2O [145].

3.2.2 Trends

In Fig. 2, all of the calculated $BDEs(M^+-OH_n)$ (M = K − La, Hf − Rn; n = 0–2) are plotted. The periodic trend is similar to that reported recently for the $BDEs(M^+-CH_2)$ (M = K − La, Hf − Rn) [105]. The M–O covalent bond of

d-block transition metals increases from the 4th row down to the 6th row, while the corresponding covalent bonds of p-block MOH_n^+ systems decrease from top to bottom. For the water complexes, in which dative bonds are mainly involved, periodic trends along the periods are not very obvious. One aspect deserves mentioning: due to the lone pair on O atom which can donate to empty orbitals of M^+, and the electronegativity difference of O and CH_2, the binding preference for O when compared with CH_2 is shifted to early transition metals and "early" p-block elements. Owing to the high oxophilicity of early transition metals, the double-humped shape of the trend for d-block elements is not so obvious. In some cases, e.g. $BDEs(M^+-O)$ (M = Y − Cd), the trend becomes single-humped. Currently, there is a lack of experimental BDE data for those MOH^+ and MOH_2^+ complexes derived from metals that belong to the 5th and the 6th row. The trend of the $BDEs(M^+-OH_n)_{exp}$ for the transition metals in the 4th row has been analyzed in detail by different groups [23, 146, 147]. A comparison between different periods may provide a more comprehensive picture [148].
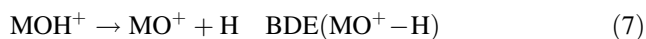
3.2.3 Hydrogen-atom affinity

As illustrated in the thermochemistry network [149] shown in Scheme 1, two other important BDEs, $BDE(MO^+-H)$ and $BDE(MOH^+-H)$, can be derived from Eqs. 7 and 8.

Fig. 2 Periodic trends in the calculated BDEs(M^+–OH_n) (in kJ mol^{-1})

Scheme 1

$$MOH^+ \rightarrow MO^+ + H \quad BDE(MO^+ - H) \tag{7}$$
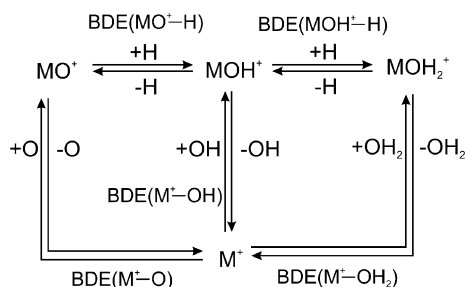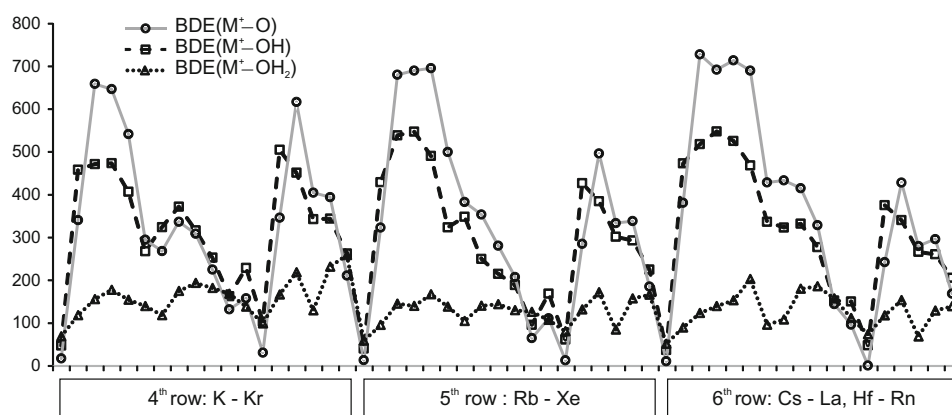
$$MOH_2^+ \rightarrow MOH^+ + H \quad BDE(MOH^+ - H) \tag{8}$$

Due to the difficulties of directly measuring BDE(MO^+–H) and BDE(MOH^+–H), these "experimental" values are derived from Eqs. 9 and 10.

$$BDE(MO^+ - H) = BDE(M^+ - OH) - BDE(M^+ - O)$$
$$+ BDE(O - H) \tag{9}$$

$$BDE(MOH^+ - H) = BDE(M^+ - OH_2) - BDE(M^+ - OH)$$
$$+ BDE(HO - H) \tag{10}$$

Although the theoretical and the experimental values for BDE(MO^+–H) and BDE(MOH^+–H) are derived from

different thermochemical cycles, the theoretical ones are in good agreement with those obtained from the experiments; for instance, the experimental values, reported by Beauchamp and co-worker, for BDE(CrO^+–H), BDE(FeO^+–H), and BDE(CoO^+–H) are 372 ± 21, 444 ± 17, and 448 ± 17 kJ mol^{-1}, respectively [150].

The BDE(MO^+–H) and BDE(MOH^+–H) are defined as the H-atom affinity (HAA) of MO^+ and MOH^+, respectively. Inspired by the remarkable periodic table of the covalent radii as proposed by Pyykkö [106–108], here we also present the H-atom affinities of MO^+ and MOH^+ in form of a periodic table (see Fig. 3). Since H-atom affinities play a prominent role in many important reactions, e.g. C–H bond activation [1, 151], water splitting [152, 153], fuel cells [154], and aerobic oxidation [155, 156], the Table in Fig. 3 might provide hints in designing new catalysts and materials. An example of using H-atom affinity has been reported quite recently [35]. In this study, we plotted the HAA of MO^+ versus the BDE(M^+–OH), which reflects the stability of MOH^+. From this figure (Fig. 1 in Ref. [35]), we concluded that the group 14 element oxides MO^+ (M = Ge, Sn and Pb) belong to the same category as MO^+ with M = Mn [157], Fe [14–17], Ca, Sr, and Ba [31]. All these binary oxides are capable to abstract a hydrogen atom from methane at room temperature. The theoretical finding suggested that GeO^+,

Fig. 3 Computed H-atom affinity of MO^+ and MOH^+ (in kJ mol^{-1})

257 — H-atom affinity of MO$^+$	kJ mol^{-1} (Eq. 7)
Ti	
183 — H-atom affinity of MOH$^+$	kJ mol^{-1} (Eq. 8)

K	Ca	Sc	Ti	V	Cr	Mn	Fe	Co	Ni	Cu	Zn	Ga	Ge	As	Se	Br	Kr
460	548	242	257	295	403	486	465	438	458	461	501	502	588	265	368	380	481
501	139	164	183	227	351	274	282	356	409	485	389	475	141	246	266	367	476
457	536	288	287	225	254	395	326	364	411	461	488	478	571	318	398	385	470
Rb	**Sr**	**Y**	**Zr**	**Nb**	**Mo**	**Tc**	**Ru**	**Rh**	**Pd**	**Ag**	**Cd**	**In**	**Sn**	**Sb**	**Te**	**I**	**Xe**
498	146	86	72	156	294	236	370	408	420	509	418	499	184	266	262	344	420
456	522	220	285	242	208	338	320	347	379	438	484	477	563	342	416	394	467
Cs	**Ba**	**La**	**Hf**	**Ta**	**W**	**Re**	**Os**	**Ir**	**Pt**	**Au**	**Hg**	**Tl**	**Pb**	**Bi**	**Po**	**At**	**Rn**
494	96	85	71	107	214	239	264	327	388	484	441	505	222	292	282	348	413

SnO^+, and PbO^+ are promising candidates as well for methane activation. In fact, this prediction was confirmed in a recent gas-phase experiment [35].

As mentioned earlier, numerous studies in the field of MOH_n^+ were conducted in sophisticated ways to understand a single subject in great a detail. In the present work, inspired by Pyykkö's studies [106–108, 158–160], we used calculations to provide an overview. We trust that Figs. 2 and 3 provide some general information that can hardly be obtained from separate measurements or calculations.

4 Conclusions

Our DFT survey on the bonding of MOH_n^+ (M = K − La, Hf − Rn; n = 0–2) can be summarized as follows:

1. Seven hybrid DFT functionals, B3LYP, BHandHLYP, M06, M06-2X, PBE1PBE, TPSSh, and X3LYP, together with the non-hybrid functional BP86, have been benchmarked with a thermochemistry database containing 50 BDEs of $M–OH_n^+$. Most of the hybrid functionals perform better than BP86 in the study. The MAE and rmsd of B3LYP, PBE1PBE, TPSSh, and X3LYP are very close to each other. With a slight advantage, B3LYP/def2-QZVP was found to be the most reliable one among the functionals tested. This method predicts $BDE(M^+–OH_n)$ with reasonable accuracy and error distributions (MAE = 19 kJ mol^{-1} and rmsd = 24 kJ mol^{-1}).

2. All tested hybrid functionals except TPSSh underestimated the BDEs, while BP86 overestimated the BDEs, as expected. For B3LYP, BHandHLYP, PBE1PBE, TPSSh, X3LYP, and BP86, the MEs linearly depend on the percentage of the exact exchange of the functionals.

3. Compared with BS-LA and BS-SDD, the Ahlrichs' new basis set, def2-QZVP, improves significantly the performance of B3LYP.

4. One hundred and sixty-two BDEs of $M^+–OH_n$ (M = K − La, Hf − Rn; n = 0–2) are calculated at B3LYP/def2-QZVP and their periodic trends are presented. By comparing the BDE_{b3lyp} and BDE_{exp}, not only existing difficulties of theory were revealed also errors in the experimental studies were indicated. At this stage, the present computationally derived results may serve as a reference for unknown BDEs with some likely errors.

5. H-atom affinities of MO^+ and MOH^+ are derived from the calculated BDEs. An application of using these properties to search for candidates for methane activation has been reviewed.

References

1. Lunsford JH (1995) Angew Chem Int Ed 34(9):970–980
2. Arndtsen BA, Bergman RG, Mobley TA, Peterson TH (1995) Acc Chem Res 28(3):154–162
3. Labinger JA (2004) J Mol Catal A Chem 220(1):27–35
4. Schröder D, Schwarz H (1995) Angew Chem Int Ed 34(18):1973–1995
5. Schwarz H, Schröder D (2000) Pure Appl Chem 72(12):2319–2332
6. O'Hair RAJ, Khairallah GN (2004) J Cluster Sci 15(3):331–363
7. Böhme DK, Schwarz H (2005) Angew Chem Int Ed 44(16):2336–2354
8. Johnson GE, Tyo EC, Castleman AW (2008) Proc Natl Acad Sci USA 105(47):18108–18113
9. Schröder D, Schwarz H (2008) Proc Natl Acad Sci USA 105(47):18114–18119
10. Schlangen M, Schwarz H (2009) Dalton Trans 46:10155–10165
11. Roithová J, Schröder D (2009) Chem Rev 110(2):1170–1211
12. Schwarz H (2010) Angew Chem Int Ed Engl (accepted)
13. Božović A, Feil S, Koyanagi G, Viggiano A, Zhang X, Schlangen M, Schwarz H, Bohme D (2010) Chem Eur J 16(38):11605–11610
14. Schröder D, Schwarz H (1990) Angew Chem Int Ed 29(12):1433–1434
15. Schröder D, Fiedler A, Hrušák J, Schwarz H (1992) J Am Chem Soc 114(4):1215–1222
16. Schröder D, Schwarz H, Clemmer DE, Chen Y, Armentrout PB, Baranov VI, Böhme DK (1997) Int J Mass Spectrom Ion Processes 161(1–3):175–191
17. Shiota Y, Yoshizawa K (2003) J Chem Phys 118(13):5872–5879
18. Wesendrup R, Schröder D, Schwarz H (1994) Angew Chem Int Ed Engl 33(11):1174–1176
19. Pavlov M, Blomberg MRA, Siegbahn PEM, Wesendrup R, Heinemann C, Schwarz H (1997) J Phys Chem A 101(8):1567–1579
20. Ryan MF, Stöckigt D, Schwarz H (1994) J Am Chem Soc 116(21):9565–9570
21. Koyanagi GK, Caraiman D, Blagojevic V, Bohme DK (2002) J Phys Chem A 106(18):4581–4590
22. Lavrov VV, Blagojevic V, Koyanagi GK, Orlova G, Bohme DK (2004) J Phys Chem A 108(26):5610–5624
23. Gong Y, Zhou M, Andrews L (2009) Chem Rev 109(12):6765–6808
24. Shiota Y, Yoshizawa K (2000) J Am Chem Soc 122(49):12317–12326
25. Nakao Y, Hirao K, Taketsugu T (2001) J Chem Phys 114(18):7935–7940
26. Gutsev GL, Andrews L, Bauschlicher CW (2003) Theor Chem Acc 109(6):298–308
27. Schofield K (2006) J Phys Chem A 110(21):6938–6947
28. Song P, Guan W, Yao C, Su Z, Wu Z, Feng J, Yan L (2007) Theor Chem Acc 117(3):407–415
29. Yao C, Guan W, Song P, Su Z, Feng J, Yan L, Wu Z (2007) Theor Chem Acc 117(1):115–122

30. Schröder D, Roithová J (2006) Angew Chem Int Ed 45(34):5705–5708
31. Božović A, Bohme DK (2009) Phys Chem Chem Phys 11(28):5940–5951
32. Feyel S, Döbler J, Höckendorf R, Beyer MK, Sauer J, Schwarz H (2008) Angew Chem Int Ed Engl 47(10):1946–1950
33. de Petris G, Troiani A, Rosi M, Angelini G, Ursini O (2009) Chem Eur J 15(17):4248–4252
34. Dietl N, Engeser M, Schwarz H (2009) Angew Chem Int Ed 48(26):4861–4863
35. Zhang X, Schwarz H (2010) ChemCatChem 2(11):1391–1394
36. Becke AD (1988) Phys Rev A 38(6):3098–3100
37. Lee C, Yang W, Parr RG (1988) Phys Rev B 37(2):785–789
38. Becke AD (1993) J Chem Phys 98(7):5648–5652
39. Becke AD (1993) J Chem Phys 98(2):1372–1377
40. Zhao Y, Truhlar D (2008) Theor Chem Acc 120(1):215–241
41. Ernzerhof M, Perdew JP (1998) J Chem Phys 109(9):3313–3320
42. Tao J, Perdew JP, Staroverov VN, Scuseria GE (2003) Phys Rev Lett 91(14):146401
43. Xu X, Goddard WA (2004) Proc Natl Acad Sci USA 101(9):2673–2677
44. Perdew JP (1986) Phys Rev B 33(12):8822–8824
45. Korth M, Grimme S (2009) J Chem Theory Comput 5(4):993–1003
46. Armentrout PB (2003) Int J Mass Spectrom 227(3):289–302
47. Rodgers MT, Armentrout PB (2004) Acc Chem Res 37(12):989–998
48. Armentrout PB, Ervin KM, Rodgers MT (2008) J Phys Chem A 112(41):10071–10085
49. Holthausen MC, Heinemann C, Cornehl HH, Koch W, Schwarz H (1995) J Chem Phys 102(12):4931–4941
50. Holthausen MC, Mohr M, Koch W (1995) Chem Phys Lett 240(4):245–252
51. Holthausen MC (2005) J Comput Chem 26(14):1505–1518
52. Baker J, Pulay P (2003) J Comput Chem 24(10):1184–1191
53. de Jong GT, Sola M, Visscher L, Bickelhaupt FM (2004) J Chem Phys 121(20):9982–9992
54. Schultz NE, Zhao Y, Truhlar DG (2005) J Phys Chem A 109(49):11127–11143
55. Quintal MM, Karton A, Iron MA, Boese AD, Martin JML (2006) J Phys Chem A 110(2):709–716
56. Furche F, Perdew JP (2006) J Chem Phys 124(4):044103–044127
57. Jensen KP, Roos BO, Ryde U (2007) J Chem Phys 126(1):014103–014114
58. Niu S, Hall MB (2000) Chem Rev 100(2):353–406
59. Harrison JF (2000) Chem Rev 100(2):679–716
60. Cramer CJ, Truhlar DG (2009) Phys Chem Chem Phys 11(46):10757–10816
61. Zhao Y, González-García N, Truhlar DG (2005) J Phys Chem A 109(9):2012–2018
62. Paier J, Marsman M, Kresse G (2007) J Chem Phys 127(2):024103–024110
63. Cramer CJ, Gour JR, Kinal A, Wloch M, Piecuch P, Moughal Shahi AR, Gagliardi L (2008) J Phys Chem A 112(16):3754–3767
64. Butschke B, Schröder D, Schwarz H (2009) Organometallics 28(15):4340–4349
65. Zhao Y, Schultz NE, Truhlar DG (2005) J Chem Phys 123(16):161103–161104
66. Zhao Y, Schultz NE, Truhlar DG (2006) J Chem Theory Comput 2(2):364–382
67. Zhao Y, Truhlar DG (2008) Acc Chem Res 41(2):157–167
68. Grimme S (2006) J Comput Chem 27(15):1787–1799
69. Schwabe T, Grimme S (2007) Phys Chem Chem Phys 9(26):3397–3406
70. Schwabe T, Grimme S (2008) Acc Chem Res 41(4):569–579
71. Weigend F, Ahlrichs R (2005) Phys Chem Chem Phys 7(18):3297–3305
72. Andrae D, Häußermann U, Dolg M, Stoll H, Preuß H (1990) Theor Chim Acta 77(2):123–141
73. Leininger T, Nicklass A, Stoll H, Dolg M, Schwerdtfeger P (1996) J Chem Phys 105(3):1052–1059
74. Metz B, Stoll H, Dolg M (2000) J Chem Phys 113(7):2563–2569
75. Peterson KA, Figgen D, Goll E, Stoll H, Dolg M (2003) J Chem Phys 119(21):11113–11123
76. Dunning TH Jr, Hay PJ (1976) In: Schaefer III HF (ed) Modern theoretical chemistry, vol 3. Plenum, New York, pp 1–28
77. Frisch MJ, Trucks GW, Schlegel HB, Scuseria GE, Robb MA, Cheeseman JR, Scalmani G, Barone V, Mennucci B, Petersson GA, Nakatsuji H, Caricato M, Li X, Hratchian HP, Izmaylov AF, Bloino J, Zheng G, Sonnenberg JL, Hada M, Ehara M, Toyota K, Fukuda R, Hasegawa J, Ishida M, Nakajima T, Honda Y, Kitao O, Nakai H, Vreven T, Montgomery J, J. A., Peralta JE, Ogliaro F, Bearpark M, Heyd JJ, Brothers E, Kudin KN, Staroverov VN, Kobayashi R, Normand J, Raghavachari K, Rendell A, Burant JC, Iyengar SS, Tomasi J, Cossi M, Rega N, Millam NJ, Klene M, Knox JE, Cross JB, Bakken V, Adamo C, Jaramillo J, Gomperts R, Stratmann RE, Yazyev O, Austin AJ, Cammi R, Pomelli C, Ochterski JW, Martin RL, Morokuma K, Zakrzewski VG, Voth GA, Salvador P, Dannenberg JJ, Dapprich S, Daniels AD, Farkas Ö, Foresman JB, Ortiz JV, Cioslowski J, Fox DJ (2009) Gaussian 09, Revision A.1. Gaussian, Inc., Wallingford CT
78. Höllwarth A, Böhme M, Dapprich S, Ehlers AW, Gobbi A, Jonas V, Köhler KF, Stegmann R, Veldkamp A, Frenking G (1993) Chem Phys Lett 208(3–4):237–240
79. Ehlers AW, Böhme M, Dapprich S, Gobbi A, Höllwarth A, Jonas V, Köhler KF, Stegmann R, Veldkamp A, Frenking G (1993) Chem Phys Lett 208(1–2):111–114
80. Pyykkö P (1988) Chem Rev 88(3):563–594
81. Hrušák J, Hertwig RH, Schröder D, Schwerdtfeger P, Koch W, Schwarz H (1995) Organometallics 14(3):1284–1291
82. Heinemann C, Schwarz H, Koch W, Dyall KG (1996) J Chem Phys 104(12):4642–4651
83. Schröder D, Schwarz H, Hrušák J, Pyykkö P (1998) Inorg Chem 37(4):624–632
84. Pyykkö P (2002) Angew Chem Int Ed Engl 41(19):3573–3578
85. Schwarz H (2003) Angew Chem Int Ed Engl 42(37):4442–4454
86. Armentrout PB (1990) Annu Rev Phys Chem 41(1):313–344
87. Armentrout PB (1991) Science 251(4990):175–179
88. Schröder D, Shaik S, Schwarz H (2000) Acc Chem Res 33(3):139–145
89. Schwarz H (2004) Int J Mass Spectrom 237(1):75–105
90. Poli R (2004) J Organomet Chem 689(24):4291–4304
91. Harvey JN (2007) Phys Chem Chem Phys 9(3):331–343
92. Harvey JN, Aschi M, Schwarz H, Koch W (1998) Theor Chem Acc 99(2):95–99
93. Landis CR, Morales CM, Stahl SS (2004) J Am Chem Soc 126(50):16302–16303
94. Keith JM, Nielsen RJ, Oxgaard J, Goddard WA (2005) J Am Chem Soc 127(38):13172–13179
95. Popp B, Wendlandt J, Landis CR, Stahl SS (2007) Angew Chem Int Ed 46(4):601–604
96. Keith JM, Goddard WA (2009) J Am Chem Soc 131(4):1416–1425
97. Popp BV, Morales CM, Landis CR, Stahl SS (2010) Inorg Chem 49(18):8200–8207
98. Lanci MP, Brinkley DW, Stone KL, Smirnov VV, Roth JP (2005) Angew Chem Int Ed Engl 44(44):7273–7276
99. Wang R, Zhang XH, Chen SJ, Yu X, Wang CS, Beach DB, Wu YD, Xue ZL (2005) J Am Chem Soc 127(14):5204–5211

100. Chen SJ, Zhang XH, Yu X, Qiu H, Yap GPA, Guzei IA, Lin Z, Wu YD, Xue ZL (2007) J Am Chem Soc 129(46):14408–14421
101. Huber S, Ertem M, Aquilante F, Gagliardi L, Tolman W, Cramer C (2009) Chem Eur J 15(19):4886–4895
102. Yu H, Fu Y, Guo Q, Lin Z (2009) Organometallics 28(15):4443–4451
103. Zhang X, Schlangen M, Baik M-H, Dede Y, Schwarz H (2009) Helv Chim Acta 92(1):151–164
104. Reiher M, Salomon O, Hess BA (2001) Theor Chem Acc 107(1):48–55
105. Zhang X, Schwarz H (2010) Chem Eur J 16(20):5882–5888
106. Pyykkö P, Riedel S, Patzschke M (2005) Chem Eur J 11(12):3511–3520
107. Pyykkö P, Atsumi M (2009) Chem Eur J 15(1):186–197
108. Pyykkö P, Atsumi M (2009) Chem Eur J 15(46):12770–12779
109. Carter EA, Goddard WA (1988) J Phys Chem 92(8):2109–2115
110. Carter EA, Goddard WA (1988) J Phys Chem 92(20):5679–5683
111. Schröder D, Schwarz H, Harvey JN (2000) J Phys Chem A 104(48):11257–11260
112. Miliordos E, Mavridis A (2007) J Phys Chem A 111(10):1953–1965
113. Miliordos E, Mavridis A (2010) J Phys Chem A 114(33):8536–8572
114. Fisher ER, Elkind JL, Clemmer DE, Georgiadis R, Loh SK, Aristov N, Sunderlin LS, Armentrout PB (1990) J Chem Phys 93(4):2676–2691
115. Armentrout PB, Kickel BL, (1996) in Organometallic Ion Chemistry, Ed. Freiser BS (Kluwer, Dordrecht, 1996) 1
116. Rodgers MT, Walker B, Armentrout PB (1999) Int J Mass Spectrom 182–183:99–120
117. Clemmer DE, Dalleska NF, Armentrout PB (1991) J Chem Phys 95(10):7263–7268
118. Dalleska NF, Armentrout PB (1994) Int J Mass Spectrom Ion Processes 134(2–3):203–212
119. Sievers MR, Chen Y-M, Armentrout PB (1996) J Chem Phys 105(15):6322–6333
120. Chen Y-M, Armentrout PB (1995) J Chem Phys 103(2):618–625
121. Murad E (1981) J Chem Phys 75(8):4080–4085
122. Hinton CS, Li F, Armentrout PB (2009) Int J Mass Spectrom 280(1–3):226–234
123. Irikura KK, Beauchamp JL (1991) J Phys Chem 95(21):8344–8351
124. Irikura KK, Beauchamp JL (1989) J Am Chem Soc 111(1):75–85
125. Zhang XG, Armentrout PB (2003) J Phys Chem A 107(42):8904–8914
126. Li FX, Gorham K, Armentrout PB (2010) J Phys Chem A 114(42):11043–11052
127. Clemmer DE, Aristov N, Armentrout PB (1993) J Phys Chem 97(3):544–552
128. Clemmer DE, Chen Y-M, Khan FA, Armentrout PB (1994) J Phys Chem 98(26):6522–6529
129. Chen Y-M, Clemmer DE, Armentrout PB (1994) J Am Chem Soc 116(17):7815–7826
130. Dzidic I, Kebarle P (1970) J Phys Chem 74(7):1466–1474
131. Kochanski E, Constantin E (1987) J Chem Phys 87(3):1661–1665
132. Magnera TF, David DE, Michl J (1989) J Am Chem Soc 111(11):4100–4101
133. Dalleska NF, Honma K, Sunderlin LS, Armentrout PB (1994) J Am Chem Soc 116(8):3519–3528
134. Schultz RH, Armentrout PB (1993) J Phys Chem 97(3):596–603
135. Koizumi H, Larson M, Muntean F, Armentrout PB (2003) Int J Mass Spectrom 228(2–3):221–235
136. Li S, Dixon DA (2007) J Phys Chem A 111(46):11908–11921
137. Bauschlicher CW, Gutsev GL (2002) Theor Chem Acc 107(5):309–312
138. Cundari TR, Harvey JN, Klinckman TR, Fu W (1999) Inorg Chem 38(24):5611–5615
139. Rue C, Armentrout PB, Kretzschmar I, Schröder D, Schwarz H (2002) J Phys Chem A 106(42):9788–9797
140. Armentrout PB, Kretzschmar I (2009) Inorg Chem 48(21):10371–10382
141. Liu F, Zhang X-G, Armentrout PB (2005) Phys Chem Chem Phys 7(5):1054–1064
142. Roithová J, Schröder D (2009) Coord Chem Rev 253(5–6):666–677
143. Lin Z (2010) Acc Chem Res 43(5):602–611
144. Schwarz J, Schröder D, Schwarz H, Heinemann C, Hrušák J (1996) Helv Chim Acta 79(4):1110–1120
145. Vukomanovic D, Stone JA (2000) Int J Mass Spectrom 202(1–3):251–259
146. Ricca A, Bauschlicher CW (1997) J Phys Chem A 101(47):8949–8955
147. Schröder D, Souvi SO, Alikhani E (2009) Chem Phys Lett 470(4–6):162–165
148. Cheng P, Koyanagi GK, Bohme DK (2007) J Phys Chem A 111(35):8561–8573
149. Schröder D (2008) J Phys Chem A 112(50):13215–13224
150. Kang H, Beauchamp JL (1986) J Am Chem Soc 108(24):7502–7509
151. Janardanan D, Wang Y, Schyman P, Que L, Shaik S (2010) Angew Chem Int Ed 49(19):3342–3345
152. Gilbert JA, Eggleston DS, Murphy WR, Geselowitz DA, Gersten SW, Hodgson DJ, Meyer TJ (1985) J Am Chem Soc 107(13):3855–3864
153. Yang X, Baik M-H (2006) J Am Chem Soc 128(23):7476–7485
154. Nørskov JK, Rossmeisl J, Logadottir A, Lindqvist L, Kitchin JR, Bligaard T, Jonsson H (2004) J Phys Chem B 108(46):17886–17892
155. Stahl SS (2004) Angew Chem Int Ed Engl 43(26):3400–3420
156. Stahl SS (2005) Science 309(5742):1824–1826
157. Ryan MF, Fiedler A, Schröder D, Schwarz H (1995) J Am Chem Soc 117(7):2033–2040
158. de Macedo LGM, Pyykkö P (2008) Chem Phys Lett 462(1–3):138–143
159. Roos BO, Pyykkö P (2010) Chem Eur J 16(1):270–275
160. Pyykkö P (2010) Phys Chem Chem Phys. doi:10.1039/C0CP01575J